Materials Science-Poland, Vol. 25, No. 3, 2007

Novel sol-gel derived films for luminescence-based oxygen and pH sensing

D. WENCEL*, C. HIGGINS, A. KLUKOWSKA, B. D. MACCRAITH, C. MCDONAGH

Optical Sensors Laboratory, National Centre for Sensor Research,
Dublin City University, Glasnevin, Dublin 9, Ireland

A range of both sol-gel and polymer derived sensor films have been developed for optical oxygen and pH sensing. Oxygen sensing is based on the luminescence quenching of the ruthenium complex [Ru(II)-tris(4,7-diphenyl-1,10-phenanthroline)]dichloride, ($[Ru(dpp)_3]^{2+}$), which is entrapped in the sol-gel matrix. The oxygen-dependent luminescence is detected using the principle of phase fluorometry, which facilitates indirect monitoring of the luminescence lifetime. The pH sensor uses excitation ratiometric detection of the fluorescence from the pH sensitive dye, 1-hydroxypyrene-3,6,8-trisulfonic acid, ion-paired with cetyl trimethyl ammonium bromide (HPTS_IP). The phase-based detection scheme, dual lifetime referencing (DLR), was also examined as an alternative sensing strategy. ORMOSIL oxygen sensor films were fabricated using a range of organosilicon precursors including methyltriethoxysilane (MTEOS), ethyltriethoxysilane (ETEOS), *n*-propyltriethoxysilane (PTEOS) and phenyltriethoxysilane (PhTEOS). In addition to optimising the sensor performance, issues such as the influence of humidity on oxygen sensing were addressed. By varying the processing parameters, the surface characteristics and microstructure were tailored to suit applications such as breath gas analysis and bioprocess monitoring. pH sensor films were prepared by hydrolyzing and co-condensing (3-aminopropyl) trimethoxysilane (APTMS) with an organosilicon monomer such as ETEOS or PTEOS or the polymer, ethyl cellulose (EC). Optimised pH sensors showed good reproducibility, reversibility and short response times. The dynamic range for these sensor films extends from pH 6.00 to 8.50 which is relevant for bioprocess monitoring applications. The spectral compatibility of the luminophores and the printability of the sol-gels present the possibility of simultaneous oxygen and pH sensing using low-cost LEDs as excitation sources along with common detection electronics.

Key words: *sol-gel; ORMOSIL; optical pH sensor; optical oxygen sensor; luminescence sensor*

1. Introduction

Luminescence-based chemical sensors have been extensively researched in recent years due to their importance in industrial, environmental, and biomedical applications [1]. These sensors combine the intrinsic sensitivity of the luminescence process with a wide availability of optoelectronic components, thereby enabling the design of a broad range of sensor configurations.

---

*Corresponding author, e-mail: Dorota.wencel2@mail.dcu.ie

Oxygen and pH are the two most important parameters in the area of continuous bioprocess monitoring [2]. Luminescence-based optical sensors for these analytes offer many advantages over conventional electrochemical sensors, as they do not suffer from electrical interference, are highly sensitive and easy to miniaturise [1]. The use of the sol-gel process when fabricating such sensors facilitates the tailoring of the structure, configuration and composition of the sensor films, thus providing a stable, transparent and permeable host matrix for the encapsulation of diverse reagents. This high degree of versatility makes sol-gel materials a more attractive alternative to organic polymers [3, 4]. In addition, the sol-gel process is compatible with a wide variety of thin film deposition techniques, for example dip-coating and spin-coating, as well as a range of printing techniques such as stamp, ink-jet and pin-printing [5–7]. Organically modified silicates (ORMOSILs) are a class of sol-gel materials that show great potential for the development of chemical sensors. In these materials, the functional group R is bound to silicon via a Si–C bond, ie., $R_{4-x}Si(OR')_x$, which is non-hydrolyzable. Through the correct choice of R, it is possible to impart specific properties such as polarity, flexibility, and porosity to the matrix [8-10].

In this paper, we report on a series of luminophore-doped ORMOSIL films, tailored for the optical detection of oxygen and pH. Oxygen sensor materials are doped with the oxygen-sensitive ruthenium complex tris(4,7-diphenyl-1,10-phenanthroline)ruthenium (II), ($[Ru(dpp)_3]^{2+}$). The pH sensor is based on a derivative of 1-hydroxypyrene-3,6,8-trisulfonic acid (HPTS), which is ion-paired with cetyl trimethyl ammonium bromide (HPTS_IP) and entrapped in a suitable matrix. Phase fluorometry and a referenced dual excitation scheme are used as detection methods for oxygen and pH sensing, respectively. These methods are insensitive to probe leaching, photobleaching, and instabilities in the light source or photodetector [11, 12].

2. Background

2.1. Oxygen sensing

The oxygen sensor described here exploits the well-known effect of oxygen quenching on the excited-state lifetime of the sol-gel-encapsulated, oxygen-sensitive luminophore $[Ru(dpp)_3]^{2+}$ [11, 13]. $[Ru(dpp)_3]^{2+}$ was selected as it has a high quantum yield, long luminescence lifetime (~5 μs) and can be excited using an inexpensive blue LED. The quenching process is described by the Stern–Volmer equation [11]:

$$\frac{I_0}{I} = \frac{\tau_0}{\tau} = 1 + K_{SV}[O_2] = 1 + k_q \tau_0 [O_2] \tag{1}$$

where I and τ are the luminescence intensity and decay time of the luminophore, respectively, and the subscript 0 denotes the absence of oxygen; K_{SV} is the Stern–Volmer constant which represents sensor sensitivity; $[O_2]$ is the concentration of oxygen; and

k_q is the bimolecular quenching constant, which incorporates the oxygen diffusion coefficient for the matrix. For homogeneous environments, the dependence of I_0/I or τ_0/τ upon $[O_2]$ yields a linear plot with a slope equal to K_{SV} and an intercept of unity. In the case of luminophores entrapped in a solid matrix, these plots deviate from the Stern–Volmer equation and become non-linear [14–16]. This behaviour is associated with the distribution of the luminophore in the solid matrix, where the embedded luminescent species encounters different environmental influences. The host microheterogeneity causes luminophore populations in different sites to be quenched differently with a resultant downward curve in the Stern–Volmer plot.

2.2. pH sensing

HPTS is a widely known pH-sensitive dye, with pKa around 7.30 that has been extensively used for fluorescence-based pH and carbon dioxide detection [17–21]. The pH-dependent absorption and emission spectra of HPTS are shown in Fig. 1.

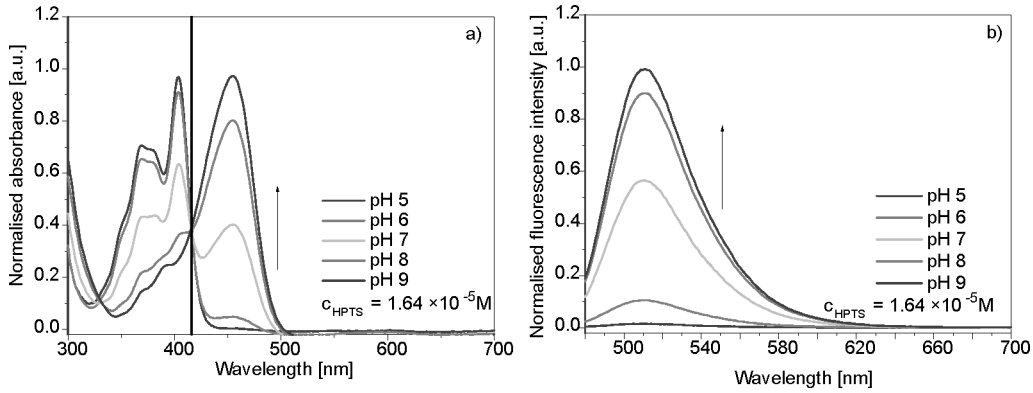

Fig. 1. Normalised absorption spectra (a) and fluorescence spectra (λ_{exc} = 470 nm) (b) of HPTS in 0.15 M phosphate buffers at various pH values

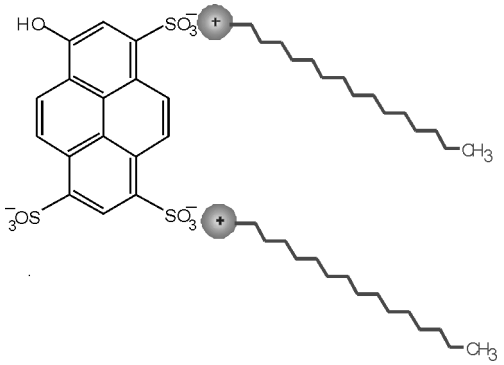

Fig. 2. Chemical structure of HPTS_IP

HPTS exhibits two absorption maxima, one at 404 nm corresponding to its acidic form, the other at 455 nm corresponding to its basic form. The emission spectra show one maximum at 510 nm. Therefore, HPTS can be used for single emission and dual excitation measurements. The excitation intensity ratio, R, defined as the emission intensity with 455 nm (blue) excitation divided by the emission intensity with 405 nm (UV) excitation ($I_{455\ nm}/I_{405\ nm}$), is related to pH [12].

In this report, we describe an optical pH sensor with a physically entrapped HPTS derivative, HPTS_IP (Fig. 2), in a variety of sol-gel and polymer matrices. HPTS_IP is more hydrophobic than HPTS and displays poor water solubility. By using such a dye, one can expect minimised leaching and improved sensor film stability. It exhibits the same pH-dependent absorption and emission maxima as the unmodified HPTS indicator.

3. Experimental

Chemical reagents. The following chemicals were purchased from Sigma Aldrich Chemicals (Ireland): tetraethoxysilane (TEOS), methyltriethoxysilane (MTEOS), ethyltriethoxysilane (ETEOS), *n*-propyltriethoxysilane (PTEOS), phenyltriethoxysilane (PhTEOS), ethyl cellulose (EC), absolute ethanol (EtOH), hydrochloric acid (HCl), HPTS, cetyl trimethyl ammonium bromide (CTAB), ruthenium (III) chloride ($RuCl_3$) and the (4,7-diphenyl-1,10-phenanthroline) ligand. (3-aminopropyl)trimethoxysilane (APTMS) and 1-methylimidazole (MI) was purchased from Fluka (Ireland). $[Ru(dpp)_3]^{2+}$was synthesised as described in the literature [22]. Glass slides were purchased from AGB Scientific Ltd.

Phosphate buffer solutions of defined pH were prepared from analytical grade potassium salts of hydrogen phosphate and dihydrogen phosphate (total concentration of phosphate 0.15 M) (Sigma Aldrich Chemicals, Ireland). Aqueous solutions were prepared from deionised (DI) water. All chemicals were used as received.

Sensor film fabrication. Oxygen sensor xerogels were prepared using the organosilicon precursors, MTEOS, ETEOS, PTEOS and PhTEOS. Sols were prepared by acid-catalyzed hydrolysis and condensation of these precursors. In a typical preparation, the precursor was combined with absolute ethanol (EtOH), followed by a dropwise addition of aqueous HCl at pH 1. The mixture was then stirred for 20 min. An ethanolic solution of $[Ru(dpp)_3]^{2+}$ was subsequently added to the sol to give a final dye concentration of 2.5 g/l with respect to the total volume of the solution. The final mixture was stirred under ambient conditions and aged for various times depending on the precursor used. The final molar ratio of silane:EtOH:water:HCl was 1:6.25:4:0.007.

In order to fabricate pH sensor films, an APTMS-derived sol was prepared by base catalysis using MI. All other aspects of APTMS sol preparation were as described above.

APTMS/ETEOS and APTMS/PTEOS composite sols were prepared by mixing the APTMS sol with the relevant precursor sol to form compositions that contained 0.1, 0.3, 0.5, 0.7 and 1 mol of APTMS. The HPTS_IP doped solutions were fabricated by mixing an ethanolic solution of the pH sensitive dye with the prepared sols to give a final silane/dye ratio of 10^{-3}. EC solutions were prepared by dissolving 5 g of the polymer in 100 ml of EtOH. The polymer-based solution was combined with the APTMS sol in a 50/50 molar ratio. Films derived from just EC were also prepared for the purpose of comparison.

All films were formed by dip-coating using a dip-speed of 3 $mm \cdot s^{-1}$ in a controlled environment using a computer-controlled dipping apparatus. The glass slides were treated with 30% HNO_3 for 24 h and then rinsed with copious amount of DI water and EtOH. After deposition, pH sensor films were cured at 140 ºC for 4 h. For the purpose of comparison, solutions of standard HPTS were also prepared and tested.

Instrumentation. The principles of phase fluorometry and the experimental system used to examine the performance of the oxygen sensors have been published previously [23, 24]. Briefly, the characterisation system consists of a blue LED (Nichia, NSPE590), which is modulated at the frequency of 20 kHz and provides excitation of the luminescent sensors. A silicon photodiode (Radionics 194-290) was used for the detection of the oxygen-sensitive luminescent signal. In order to examine their performance, oxygen sensor films were placed in a flow cell into which controlled mixtures of oxygen and nitrogen were flowed using mass flow controllers (Celerity, Ireland).

The pH fluorescence measurements were acquired using a FluoroMax-2 fluorometer (Jobin Yvon, USA). All spectra were recorded in a quartz cuvette fixed at 45º with respect to the incident beam. Films on the glass slides were immersed in phosphate buffer solutions adjusted to pH values ranging from 4.00 to 10.00. The fluorometer collected the emission intensity at 515 nm, employing excitation wavelengths of 405 nm and 455 nm. 2 nm passbands were used for both the excitation and emission monochromators. The pH values were verified with a commercial pH meter (Orion Benchtop 420 A+, USA.). All measurements were performed at room temperature.

Frequency domain dual lifetime referenced (DLR) measurements were performed using a dual phase lock-in amplifier (DSP 7225 Perkin Elmer Instruments, USA). This provided sinusoidal modulation of the LED and phase-shift detection of the photodiode output signal.Contact angle measurements were made using an FTA-200 contact angle analyzer (First Ten Angstroms, USA) by imaging a droplet of water that was dispensed onto the surface being characterised. The captured images were then analysed using dedicated software. The oxygen diffusion coefficient within the films was determined as a means to establish the origin of the observed oxygen sensitivity. This was achieved, as reported previously, by measuring the response time, t_{90}, for films of known thickness [25]. Diffusion coefficients were then recovered from the response time data via the Schappacher–Hartmann protocol [26]. Film thickness measurements were obtained using a white light interferometer (WYKO NT1100 Optical Profiling System, Veeco, USA).

4. Results and discussion

4.1. Oxygen sensor films with enhanced sensitivity

All oxygen sensor films exhibit excellent repeatability, reversibility, and fast response times (less than 1 s). An example of an ETEOS-derived oxygen sensor response is shown in Fig. 3.

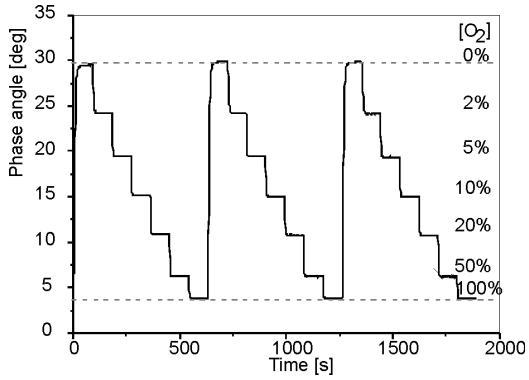

Fig. 3. Phase response for an ETEOS-derived film, doped with $[Ru(dpp)_3]^{2+}$

A linear Stern–Volmer plot indicates that the entrapped luminophore population reports from a homogeneous microenvironment. Strictly linear Stern–Volmer behaviour seems to be an exception as most solid oxygen sensors give non-linear curves, as discussed before. Various models have been developed and used to describe such responses [14–16]. In this study, the Stern–Volmer plots were analyzed using two models: the single-site Stern–Volmer model (Eq. (1)) and the two-site Demas model (Eq. (2)):

$$\frac{I_0}{I} = \frac{\tau_0}{\tau} = \left[\frac{f_1}{1 + K_{SV1}\, pO_2} + \frac{f_2}{1 + K_{SV2}\, pO_2} \right]^{-1} \tag{2}$$

where f_1 and f_2 denote fractional distribution of the total emission from the luminophore located at different sites, 1 and 2, respectively. K_{SV1} and K_{SV2} are the Stern –Volmer quenching constant for these sites.

The model is based on the assumption that the luminophore is distributed in the solid matrix at two different sites and that each fraction has a different quenching constant. Sensors were stored for 4 weeks in the dark prior to experiments, the results of which are shown in Fig. 4.

The fit to the Demas model was excellent for all films (r^2 = 0.999). Moreover, Stern–Volmer plots for ETEOS-, PTEOS- and PhTEOS-derived sensor platforms were also quite well described by Eq. (1) ($r^2_{\mathrm{ETEOS}} = 0.985$, $r^2_{\mathrm{PTEOS}} = 0.981$, $r^2_{\mathrm{PhTEOS}} = 0.989$). This would allow a simple two-point calibration of these sensors if desired.

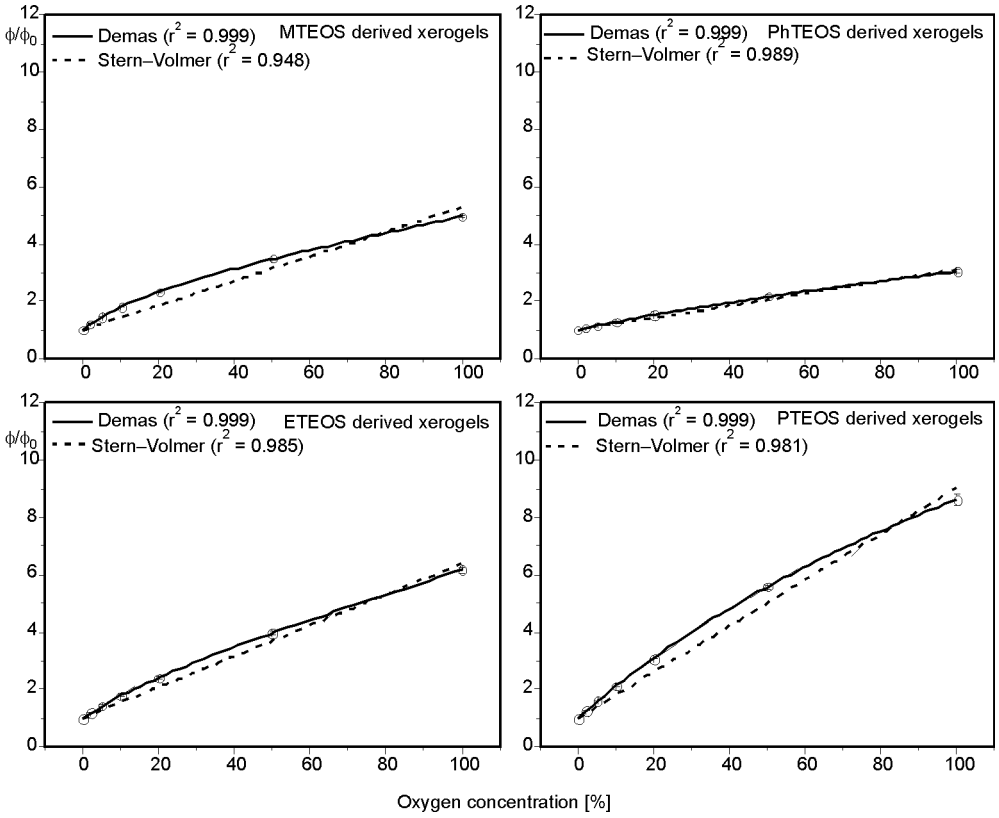

Fig. 4. Best fit to the Stern–Volmer and Demas models for various ORMOSIL oxygen sensor films

All sensors exhibit different sensitivities, as indicated by their respective K_{SV} values (Table 1). PTEOS-based films display the greatest sensitivity, with ETEOS, MTEOS, PhTEOS decreasing in oxygen sensitivity in that order. PhTEOS-derived films are the least sensitive due to the steric effect of the phenyl group. It has been demonstrated previously that films with increased hydrophobicity exhibit higher oxygen sensitivity, both in gas and dissolved phase [27]. Table 1 shows that there is a good correlation between K_{SV} and both the measured diffusion coefficients (D) and water contact angles (CA).

Table 1. Properties of ORMOSIL sensor films

Film	K_{SV} ($[O_2]^{-1}$)	CA [deg]	D [$cm^2 \cdot s^{-1}$]
PhTEOS	0.0212 ± 0.0007	93 ± 1	3.0×10^{-9}
MTEOS	0.0429 ± 0.0029	90 ± 1	9.9×10^{-7}
ETEOS	0.0540 ± 0.0020	97 ± 2	6.2×10^{-6}
PTEOS	0.0806 ± 0.0034	100 ± 1	6.7×10^{-6}

Clearly, the most hydrophobic films are PTEOS- and ETEOS-based xerogels with water contact angles of $100^o \pm 1^o$ and $97^o \pm 2^o$, respectively. High water contact angle measurements show that these coatings have a hydrophobic surface and are highly water-repellent. As such, these coatings are less prone to humidity interference than for example, MTEOS-based coatings. Figure 5 shows calibration curves for MTEOS- and ETEOS-derived oxygen sensor films recorded using dry and humidified gases. Figure 5b clearly demonstrates the humidity insensitivity of ETEOS-based oxygen sensors.

The parameters *CA*, *D*, and K_{SV} in Table 1 increase as the alkyl chain length increases. The sensitivity of PTEOS-derived films is twice that of MTEOS-based films. We can attribute the enhanced sensitivity to the increase of oxygen transport within the ETEOS- and PTEOS-derived oxygen films, as evidenced by the diffusion coefficients recorded for these films. The extension of this work will involve a study of the decay times of $[Ru(dpp)_3]^{2+}$ in these films. This, coupled with the diffusion coefficient data, will help to further elucidate the origins of film sensitivity, as K_{SV} depends not only on k_q but also on τ_0.

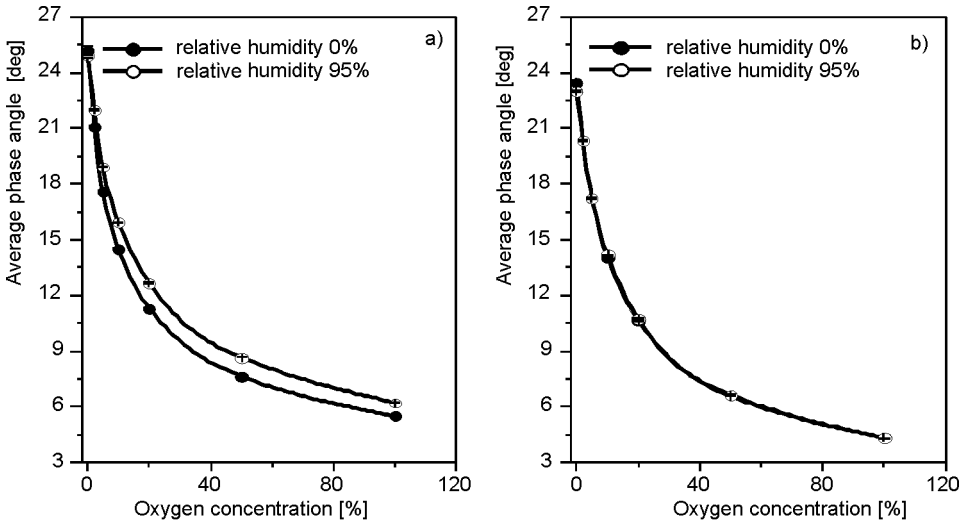

Fig. 5. Humidity interference for MTEOS- and ETEOS-derived films (error bars are within the symbols)

The ETEOS- and PTEOS-derived oxygen-sensitive films reported here are suitable for industrial and medical applications such as bioprocess management or breath monitoring, where the key sensor characteristics are: enhanced oxygen sensitivity and insensitivity to humidity.

4.2. Characterisation of the pH sensor

4.2.1. Dual excitation pH sensor

A range of sol-gel and polymer matrices were prepared in the course of this study. Both single (APTMS, ETEOS, PTEOS, EC) and binary systems (APTMS/ETEOS, APTMS/PTEOS and EC/APTMS) were prepared as described in section 3.3 and doped with HPTS_IP. Films were cured at 140 ºC. This high curing temperature was necessary, as pH sensor films for bioprocess monitoring should be autoclavable, usually at 121 ºC. Curing them at a temperature higher than that used during sterilisation minimises any structural changes of the sol-gel material. An important aspect of this work was to develop a sol-gel host matrix formulation that would give a satisfactory pH response after curing at 140 ºC.

Single and EC-based systems did not yield promising results. APTMS-, EC- and APTMS/EC-based films showed good sensitivity but poor adhesion and a high degree of leaching. In addition, the matrix became optically opaque after one pH cycle. ETEOS- and PTEOS-derived matrices display poor ion permeability as they are very hydrophobic, making them ill-suited to this application.

Binary systems represent a much better alternative, the most promising results being achieved by using a formulation comprising APTMS and PTEOS in a 50/50 molar ratio (formulation AP). Such sensors demonstrated good sensitivity and short response time after curing at 140 ºC. This is thought to be due to increased porosity and better accessibility of the dye in the material when compared to APTMS/ETEOS systems.

The excitation and emission spectra of the AP xerogel in a pH 7.00 buffer solution are shown in Fig. 6. The same spectra for HPTS in solution are also shown for comparison. As the dyes are closely related, the spectra are almost identical, the most notable difference being the fact that the excitation maxima of HPTS-IP, entrapped in the sol-gel film, are slightly red-shifted.

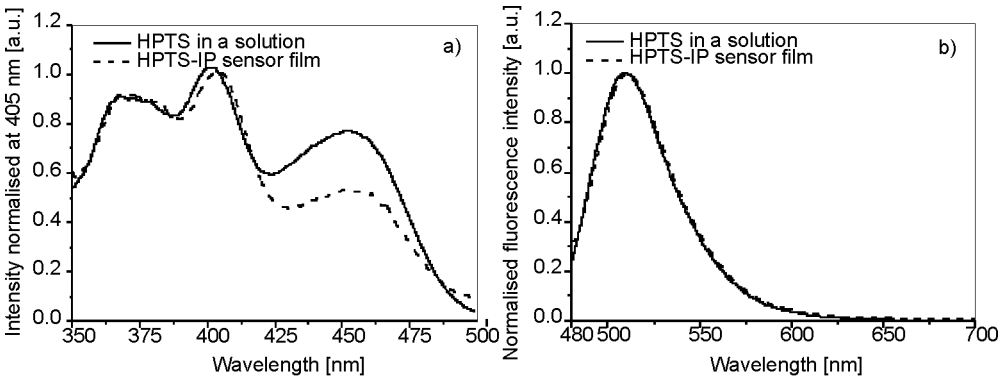

Fig. 6. Normalised excitation spectra (λ_{em} = 515 nm) (a) and emission spectra (λ_{exc} = 470 nm) (b) of 1.64×10^{-5} M HPTS solution and HPTS_IP based AP sensor xerogel in 0.15 M phosphate buffer at pH 7.00

The pH-dependent excitation spectra of the AP xerogel, normalised to intensity at 405 nm, are shown in Fig. 7. The calibration plot for this sensor film is shown in Fig. 8.

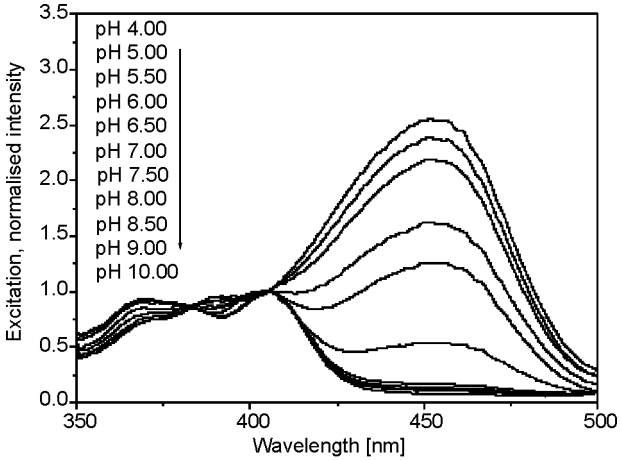

Fig. 7. Normalised excitation spectra (λ_{em} = 515 nm) of the AP sensor film at various pHs

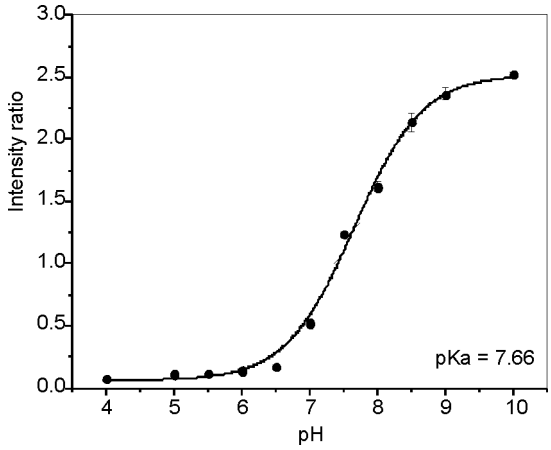

Fig. 8. Calibration plot of the AP sensor film; intensity ratios at λ_{exc}= 455 nm /λ_{exc} = 405 nm

The calculated pK_a of the entrapped dye is 7.66, which is slightly higher than that for HPTS in solution (pK_a = 7.38). This indicates an apparent reduction in pH within the matrix. The sensor dynamic range extends from approximately pH 6.00 to 8.50 which is suitable for bioprocess monitoring applications [28, 29].

The sensor response is reversible and displays negligible drift, as shown in Fig. 9. The response time for a 90% change was approximately 2.5 min from pH 6.00 to 8.00

and about 3.3 min from pH 8.00 to 6.00. The response time could be further improved by fabricating thinner films (i.e., by using a slower dip-coating speed).

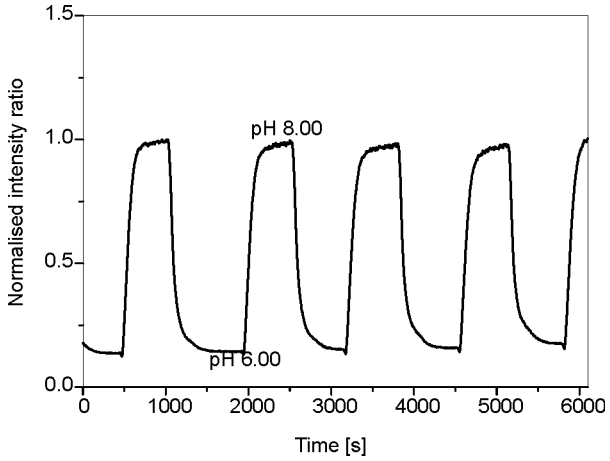

Fig. 9. Reversibility of the AP sensor film;
intensity ratios at λ_{exc}= 455 nm /λ_{exc} = 405 nm

For leaching studies, AP sensor films were soaked in pH 5.00 buffer solutions for a period of 2 weeks. With the exception of the first 24 h, during which 19% of the loosely incorporated dye leached out, no significant leaching was observed over the 2 week period, as verified using UV-Vis absorption studies. In contrast, single ORMOSIL compositions showed much higher degrees of leaching within shorter periods of time. The improved stability may be attributed to the functional groups incorporated into the sol-gel film.

Future work will involve investigation of sensor sensitivity to ionic strength, temperature, and the ability of the sensor to withstand steam sterilization.

4.2.2. DLR optical pH sensor

The principle of DLR involves the use of two luminophores (an indicator and a reference) with different decay times and similar spectral properties, to obtain a referenced, phase-based measurement of an analyte. This is described in detail elsewhere [30, 31]. In this study, the short-lived pH sensitive fluorophore, HPTS-IP, was combined with the long-lived standard, $[Ru(dpp)_3]^2$ in a sol-gel matrix.

Figure 10 displays the pH-dependent phase shifts of TEOS-derived films cured at 70 ºC and 140 ºC for 24 h, which were fabricated as described for acid-catalysed sols. The dynamic range of the film cured at 140 ºC was about 1.5 times lower than of the film cured at 70 ºC. This is due to the fact that curing at higher temperatures produces a denser oxide network and the encapsulated pH dye is therefore less accessible to protons.

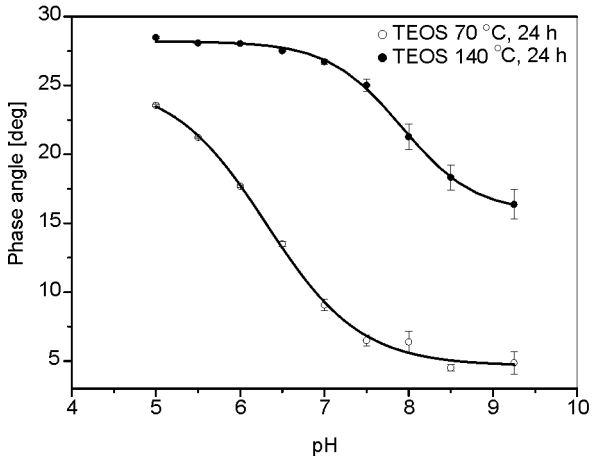

Fig. 10. Calibration plot of TEOS-based pH sensor films measured using the DLR technique

The aim of this study was to investigate the compatibility of the pH sensor with both detection techniques: dual excitation and DLR. The DLR technique is advantageous over the dual excitation technique as it requires a single LED excitation source.

5. Conclusions

Phase fluorometric ORMOSIL oxygen sensor films, doped with $[Ru(dpp)_3]^{2+}$ exhibit enhanced oxygen sensitivity. The sensitivity was correlated with the alkyl chain length of the organosilicon precursor, with the highest sensitivity being achieved for PTEOS -derived sensor films. The variation in sensitivity arises from different values of k_q in each xerogel. In this way, one can tune the sensitivity of the sensor to suit the application.

pH sensor films were based on entrapped HPTS_IP in a sol-gel matrix. HPTS_IP has the same spectral characteristics as HPTS, allowing dual excitation detection and having sensitivity in the physiological pH range, which makes such a sensor a potential candidate for use in bioprocess management. The sensor films displayed a reversible response, short response times (2.5 min) and a dynamic range extending from pH 6.00 to 8.50. The use of a lipophilic dye, which minimized leaching from the host matrix, resulted in stable pH sensor films. This sensor is also compatible with the DLR sensing technique, its advantage being the ability to provide a referenced sensor output, using a single excitation source.

Optical sensing systems for oxygen and pH sensing have been presented, which have potential for multianalyte platform measurements using inexpensive, commercially available LEDs as excitation sources and a simple detection system. These sensors have potential applications in bioprocess monitoring. In addition, the developed oxygen sensor films are compatible with breath gas analysis for human health monitoring.

References

[1] WOLFBEIS O.S., *Fiber Optic Chemical Sensors and Biosensors*, Vol. 1, CRC, Boca Raton, 1991.
[2] KOSTOV Y., HARMS P., RANDERS-EICHHORN L., RAO G., Biotech. Bioeng., 72 (2001), 346.
[3] AVNIR D., Acc. Chem. Res., 28 (1995), 328.
[4] COLLINSON M.M., HOWELLS A .R., Anal. Chem., 72 (2000), 702A
[5] BRINKER J., SCHERER G.W., *Sol-Gel Science: The Physics and Chemistry of Sol-Gel Processing*, Academic Press, New York, 1990.
[6] CARTER C.J., ALVIS R.M., BROWN S.B., LANGRY K.C., WILSON T.S., MCBRIDE M.T., MYRICK M.L., COX W.R., GROVE M.E., COLSTON B.W., Bios. Bioelec., 21 (2006), 1359.
[7] CHO E.J., BRIGHT F.V., Anal. Chim. Acta, 470 (2002), 101.
[8] LEV O., TSIONSKY M., RABINOVICH L., GLEZER V., SAMPATH S., PANKRATOV I., GUN J., Anal. Chem., 67 (1995), 22A.
[9] COLLINSON M.M., Microchim. Acta, 129 (1998), 145.
[10] LAVIN P., MCDONAGH C.M., MACCRAITH B.D., J. Sol-Gel Tech., 13 (1998), 641.
[11] LAKOWICZ J.R., *Principles of Fluorescence Spectroscopy*, Kluwer Academic Plenum Publishers, New York, 1999.
[12] VALEUR B., *Molecular Fluorescence*. *Principles and Applications***,** VCH Wiley, Weinheim, 2002.
[13] TRETTNAK W., *Optical sensors based on fluorescence quenching*, [in:] *Fluorescence Spectroscopy*. *New Methods and Applications*, O.S. Wolfbeis (Ed.), Springer Verlag, Berlin, 1992, p. 79.
[14] BACON J.R., DEMAS J.N., Anal. Chem., 59 (1987), 2780.
[15] CARRAWAY E.R., DEMAS J.N., DEGRAFF B.A., BACON J.R., Anal. Chem., 63 (1991), 337.
[16] XU W., MCDONOUGH R.C., LANGSDORF B., DEMAS J.N., DEGRAFF B.A., Anal. Chem., 66 (1994), 4133.
[17] WOLFBEIS O.S., FURLINGER E., KRONEIS H., MARSONER H., Fresenius Z. Anal. Chem., 314 (1983), 119.
[18] SCHULMAN S.G., CHEN S., BAI F., LEINER M.J.P., WEIS L., WOLFBEIS O.S., Anal. Chim. Acta, 304 (1995), 165.
[19] ZHANG S., TANAKA S., WICKRAMASINGHE Y.A.B.D., ROLFE P., Med. Biol. Eng. Comp., 33 (1995), 152.
[20] WOLFBEIS O.S., KOVACS B., GOSWAMI K., KLAINER S.M., Mikrochim. Acta 129 (1998), 181.
[21] MILLS A., CHANG Q., Analyst, 118 (1993), 839.
[22] WATTS R.J., CROSBY G.A., J. Am. Chem. Soc., 93 (1971), 3184.
[23] MCDONAGH C., KOLLE C., MCEVOY A.K., DOWLING D.L., CAFOLLA A.A., CULLENA S.J., MACCRAITH B.D., Sens. Act. B, 74 (2001), 124.
[24] WENCEL D., HIGGINS C., GUCKIAN A., MCDONAGH C., MACCRAITH B.D., Proc SPIE, 5826 (Dublin), (2005), 696.
[25] MCDONAGH C., BOWE P., MONGEY K., MACCRAITH B.D., J. Non-Cryst. Solids, 306 (2002), 138.
[26] SCHAPPACHER G., HARTMANN P., Anal. Chem., 75 (2003**)**, 4319.
[27] MCDONAGH C., MACCRAITH B.D., MCEVOY A.K., Anal. Chem., 70 (1998), 45.
[28] KERMIS H.R., KOSTOV P., HARAS Y., RAO G., Biotechnol. Prog., 18 (2002), 1047.
[29] KERMIS H.R., KOSTOV Y., RAO G., Analyst, 128 (2003), 1181.
[30] VON BÜLTZINGSLÖWEN C., MCEVOY A.K., MCDONAGH C., MACCRAITH B.D., KLIMANT I., KRAUSE C., WOLFBEIS O.S., Analyst, 127 (2002), 1478.
[31] HUBER C., KLIMANT I., KRAUSE C., WOLFBEIS O.S., Anal. Chem., 73 (2001), 2097.

Received 22 June 2006
Revised 8 March 2007